

Surface and Subsurface MVA

FWP FE-10-0001

Samuel M. Clegg, Kristy Nowak-Lovato, Julianna
Fessenden-Rahn, Ron Martinez, Robert Currier, Steve
Obrey, and Lianjie Huang

Los Alamos National Laboratory

sclegg@lanl.gov, (505)664-0403

U.S. Department of Energy
National Energy Technology Laboratory
Carbon Storage R&D Project Review Meeting
Transforming Technology through Integration and Collaboration
August 18-20, 2015

Presentation Outline

- Project Overview
 - Goals and Objectives
- Benefit to the Program
- Technical Status
 - Surface MVA
 - Subsurface MVA
- Accomplishments to Date
- Summary

Benefit to the Program

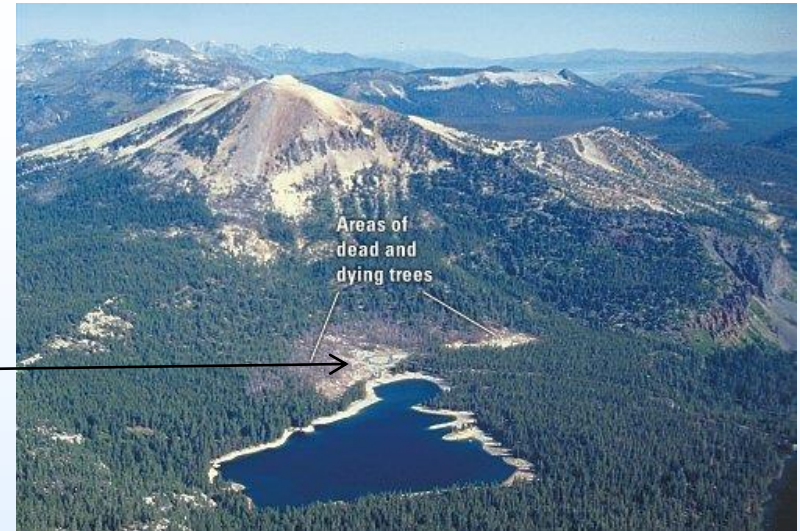
- Support industry's ability to predict CO₂ storage capacity in geologic formations to within ±30 percent.
 - Advanced Seismic Reservoir Imaging
- Develop and validate technologies to ensure 99% storage permanence.
 - FMS CO₂, H₂S, and CH₄ Monitoring
 - Advanced Seismic Reservoir Imaging
- Develop technologies to improve reservoir storage efficiency while ensuring containment effectiveness.
 - FMS CO₂, H₂S, and CH₄ Monitoring
 - Advanced Seismic Reservoir Imaging
- **Develop Best Practice Manuals for** monitoring, verification, accounting, and assessment; site screening, selection and initial characterization; **public outreach**; well management activities; and risk analysis and simulation.
 - FMS CO₂, H₂S, and CH₄ Monitoring
 - Advanced Seismic Reservoir Imaging

Project Overview: Goals and Objectives

- Surface MVA – Frequency Modulated Spectroscopy
 - Quantitatively identify CO₂, H₂S and CH₄ seepage from geologic sequestration sites
 - Distinguish anthropogenic CO₂ from natural CO₂ emissions
 - CO₂ carbon stable isotope measurements
 - H₂S sulfur and CH₄ carbon stable isotope measurements
 - Real-time remote and in situ CO₂, H₂S and CH₄ monitoring
 - Integrated into Single Instrument
- Subsurface MVA – Advanced Seismic Imaging
 - Improve velocity models for microseismic imaging
 - Improve the location precision of microseismic events

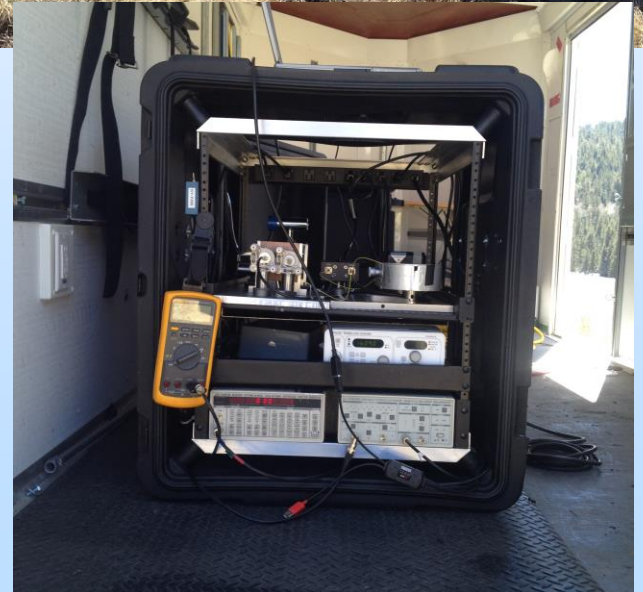
MVA Field Experiments

- 2009 - 2015 Field Experiments
 - Mammoth Springs, CA
 - Valles Caldera, NM
 - Sevilleta Long Term Ecological Research, NM
 - Farmington, NM
 - Soda Springs, UT
 - LANL Juniper-Pinon Field Site
 - ZERT, MSU, Bozeman, MT
 - Controlled CO₂ Flow & Release Rate
 - Southwest Regional Partnership, Kansas



LANL MVA Program

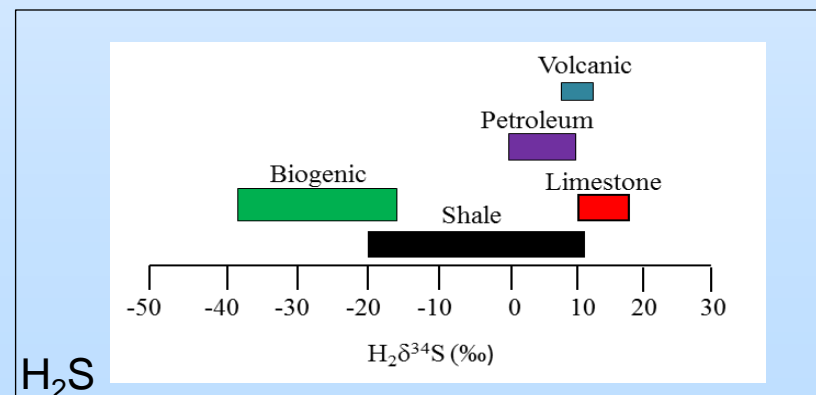
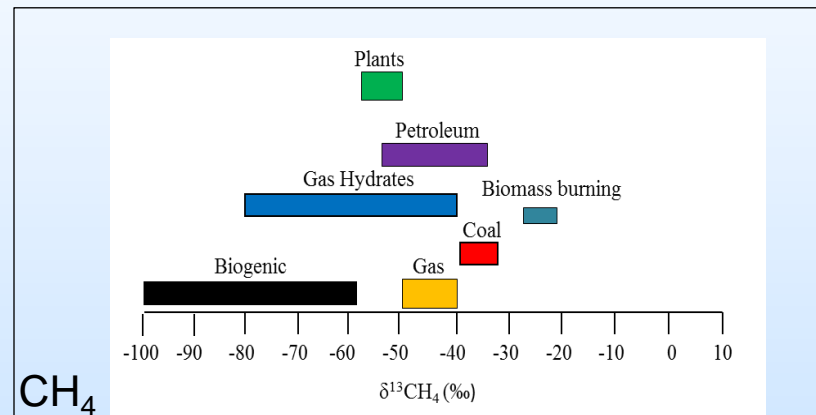
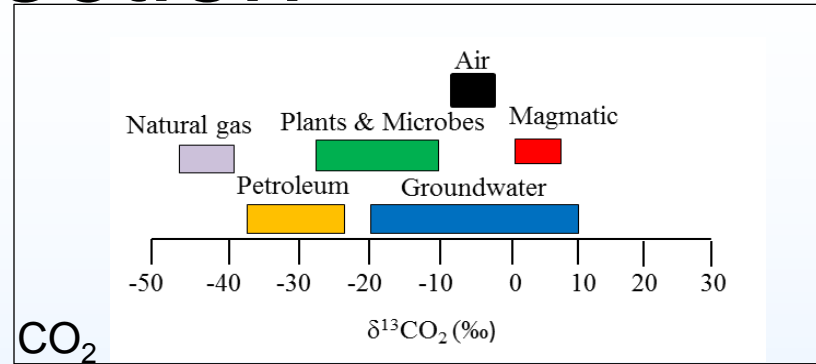
- Frequency Modulated Spectroscopy
 - In situ
 - Remote
 - LIDAR
 - CO₂, CH₄, H₂S (isotopes)
- Flask Collects, Mass Spectroscopy
- Water Stable Isotope Analysis



Stable Isotope Detection

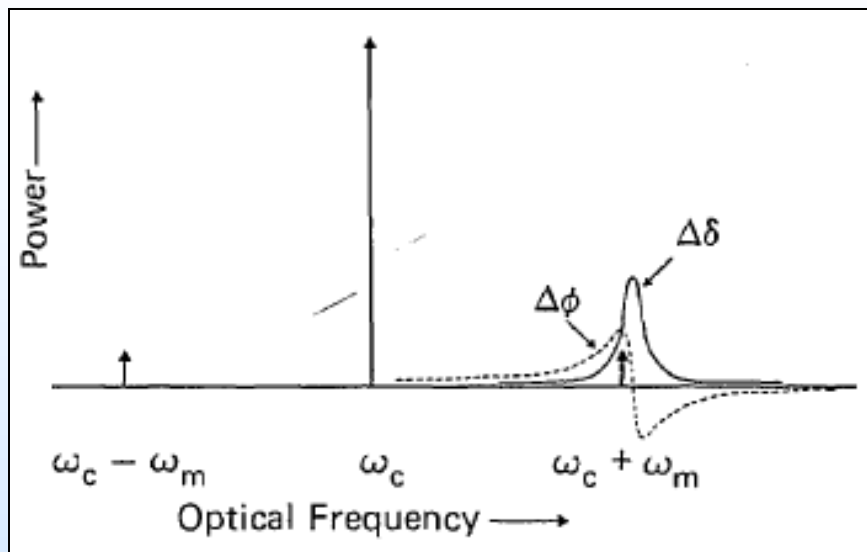
- Detect Seepage of CO₂, CH₄, H₂S at sequestration sites
- Isotopic Signatures for source identification
- Frequency Modulated Spectroscopy
 - 100x to 1000x more sensitive than absorption spectroscopy
- Generally, the Atmosphere Contains
 - 98.9% ¹²C¹⁶O₂
 - 1.1% ¹³C¹⁶O₂
- Calibration Gases Prepared In House
 - Available vendors were too expensive and took too long

$$\delta^{13}C_{sam} = \left(\frac{^{13}C_{sam}/^{12}C_{sam}}{^{13}C_{std}/^{12}C_{std}} - 1 \right) \times 1000$$

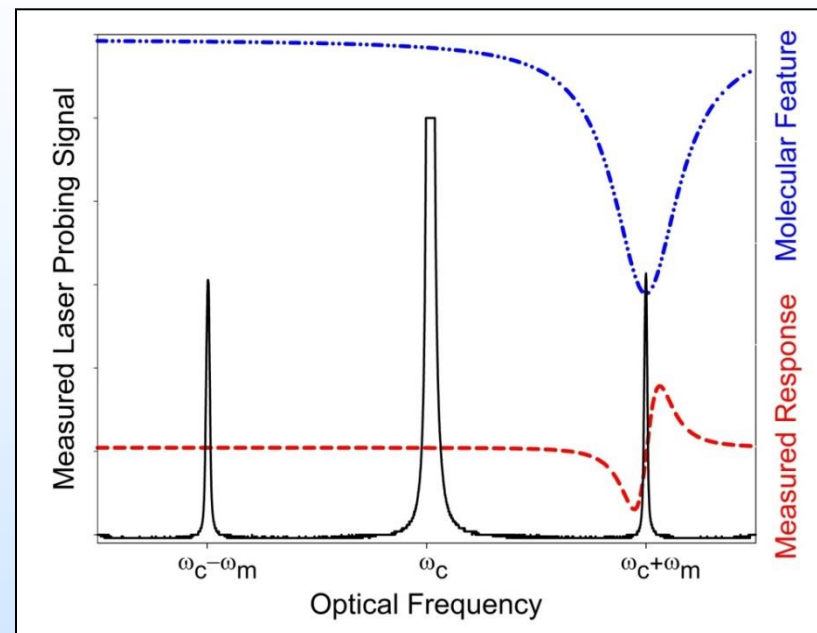


Frequency Modulated Spectroscopy

From G.C. Bjorklund Optics Letters, 5, 15, 1980



Frequency Modulation Spectroscopy



Absorption Spectroscopy Maximum Line Strengths (HITRAN)

$$^{12}\text{C}^{16}\text{O}_2 = 1.83 \times 10^{-23}$$

$$^{13}\text{C}^{16}\text{O}_2 = 2.10 \times 10^{-25}$$

$$^{12}\text{CH}_4 = 1.00 \times 10^{-21}$$

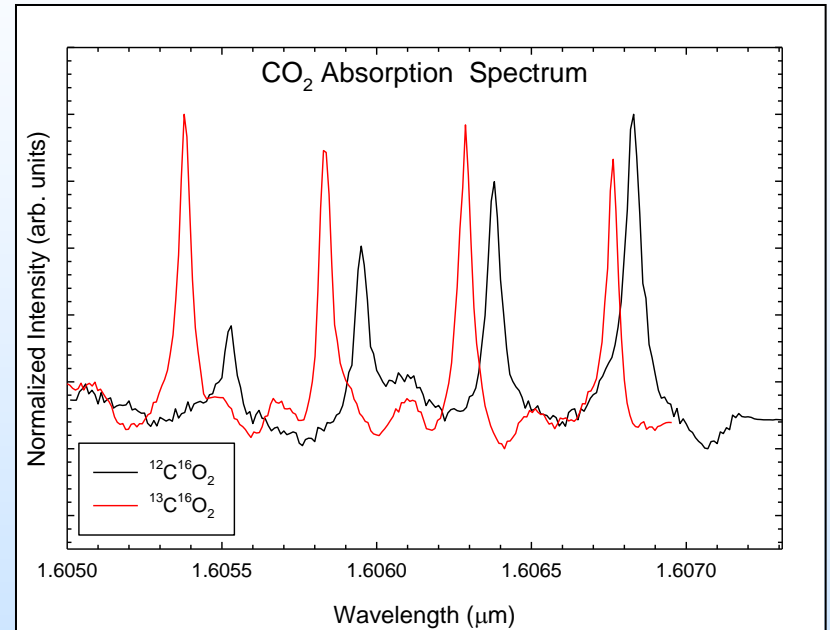
$$^{13}\text{CH}_4 = 1.59 \times 10^{-23}$$

$$\text{H}_2^{32}\text{S} = 1.3 \times 10^{-22}$$

$$\text{H}_2^{34}\text{S} = 1.8 \times 10^{-24}$$

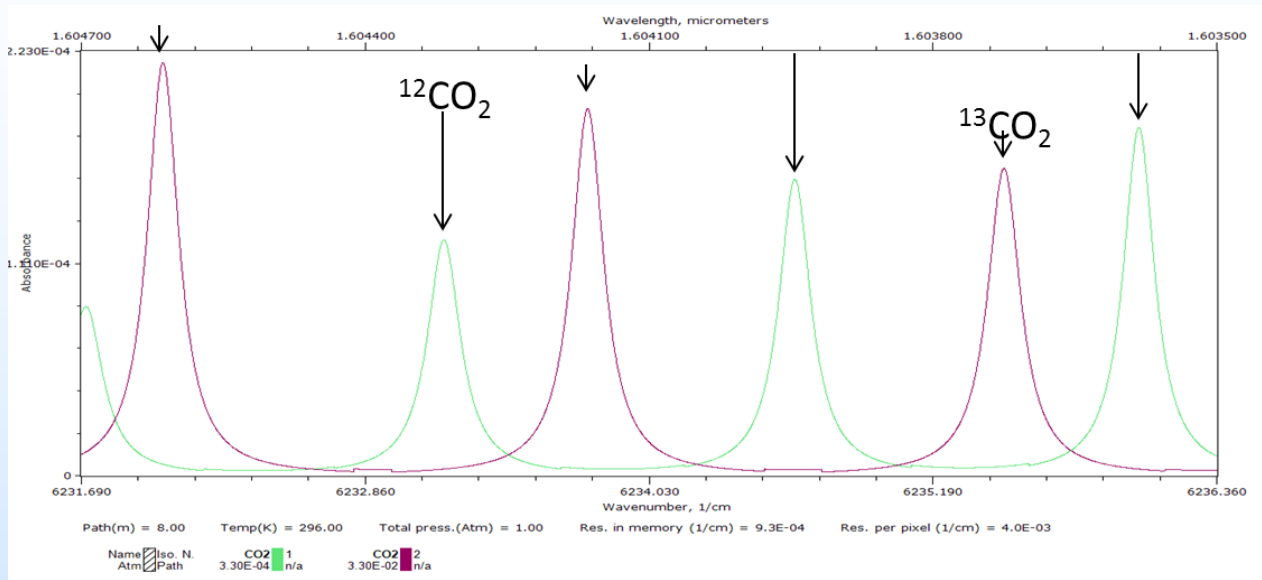
Frequency Modulated Spectroscopy

- Why 1570 – 1680nm range?
 - Telecom Electronics (1550nm)
 - Absorption Cross Section for Remote (hundreds of meters)
 - No spectral interferences.
 - H₂O or CO
- Why 1604 – 1609nm range?
 - ¹³C¹⁶O₂ Peaks between ¹²C¹⁶O₂ Sub-Bandheads.
 - ¹²C¹⁶O₂ Peaks ~10x ¹³C¹⁶O₂
 - Multiple species detection with same hardware

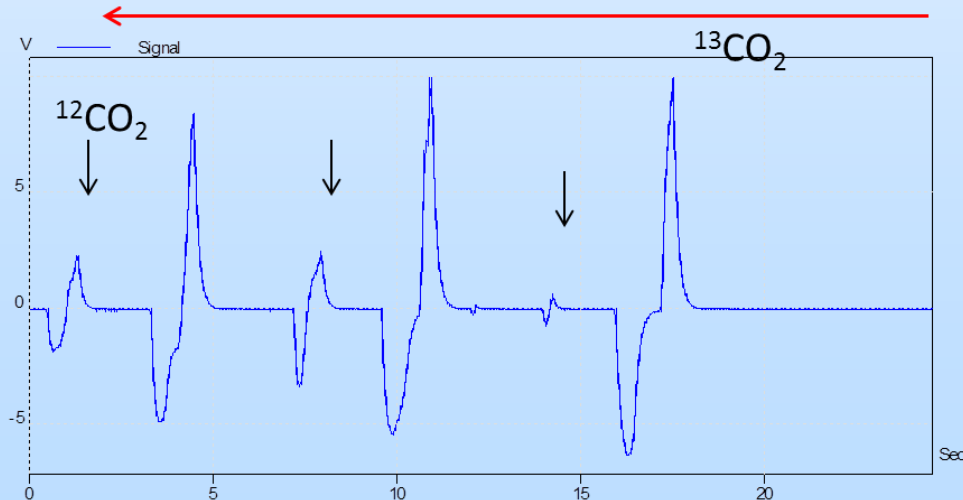


FMS Compared to HITRAN

FMS Spectra of 99% $^{13}\text{CO}_2$ with 1.0% $^{12}\text{CO}_2$

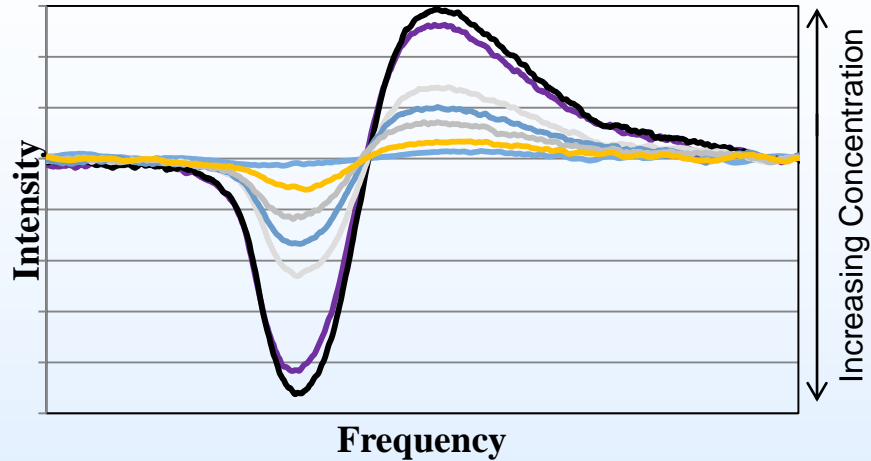


$1603.5\text{-}1604.7 \text{ cm}^{-1}$



Carbon Dioxide Calibration

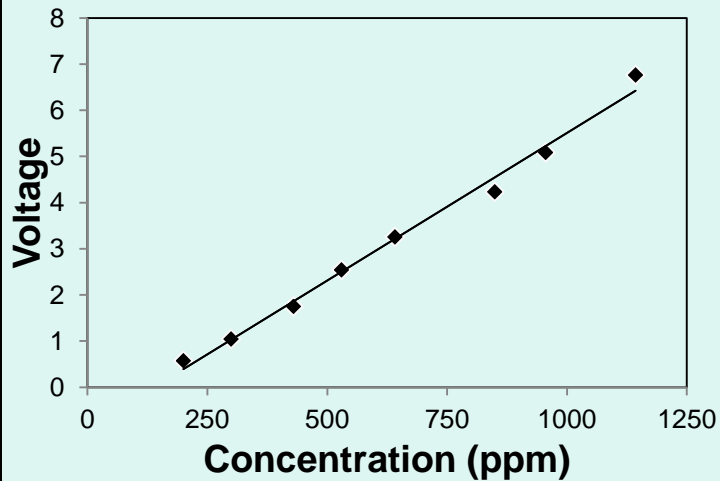
Carbon Dioxide



Estimated Detection Limit
 $^{12}\text{CO}_2$ and $^{13}\text{CO}_2 < 1$ ppb

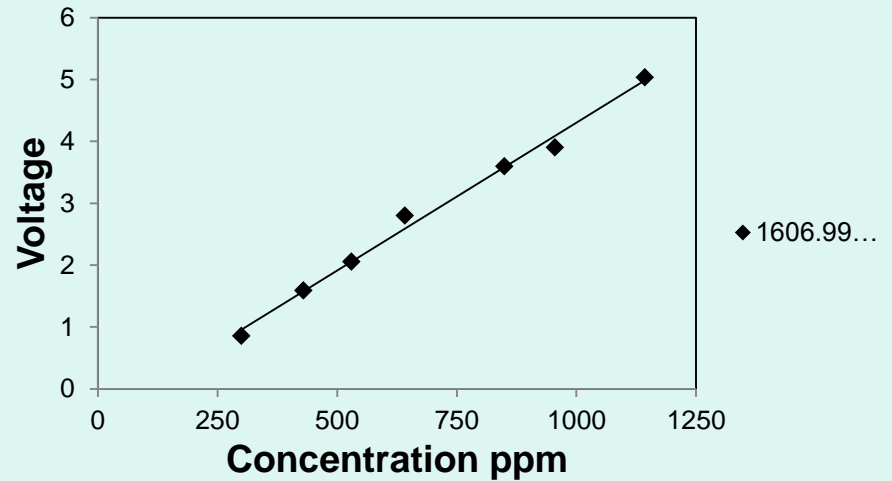
$^{12}\text{CO}_2$ Calibration

$R^2 = 0.991$



$^{13}\text{CO}_2$ Calibration

$R^2 = 0.9928$



In Situ FMS Observations

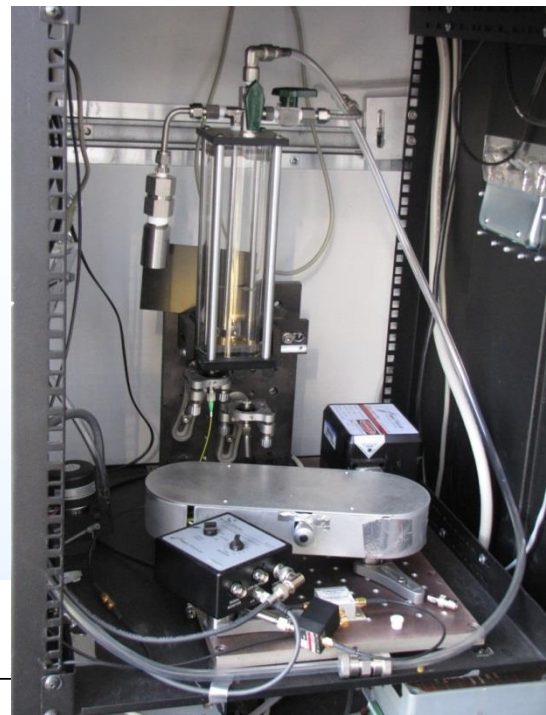
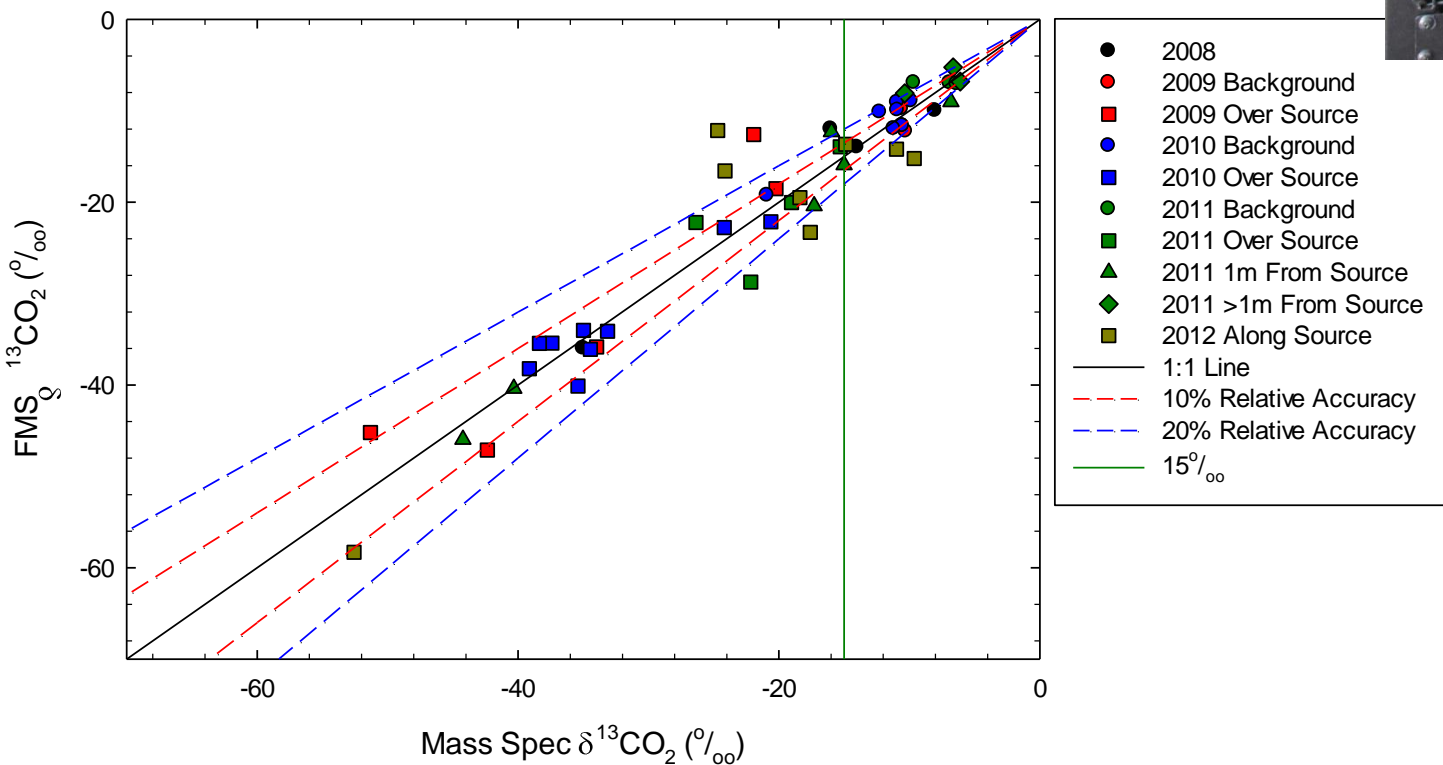
Historical Trends

Background $> -15 \text{ ‰}$

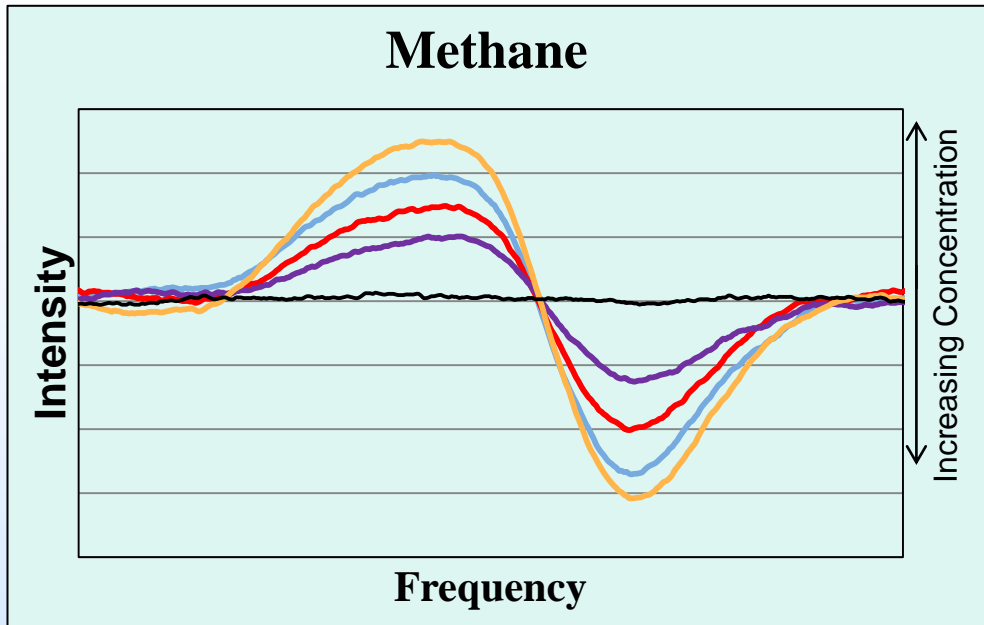
Most $> -10 \text{ ‰}$

3 observations $< -10 \text{ ‰}$

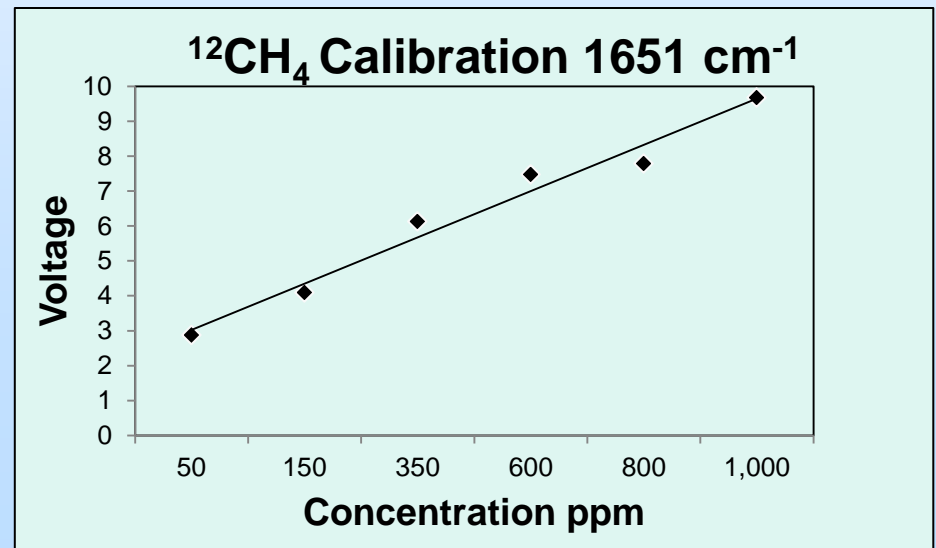
Seepage $< -15 \text{ ‰}$



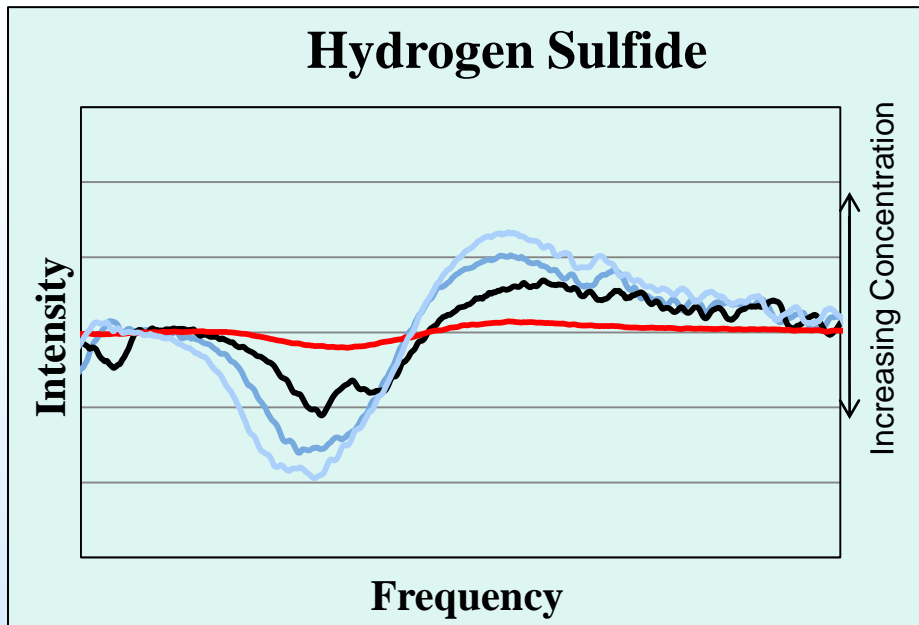
Methane Calibration



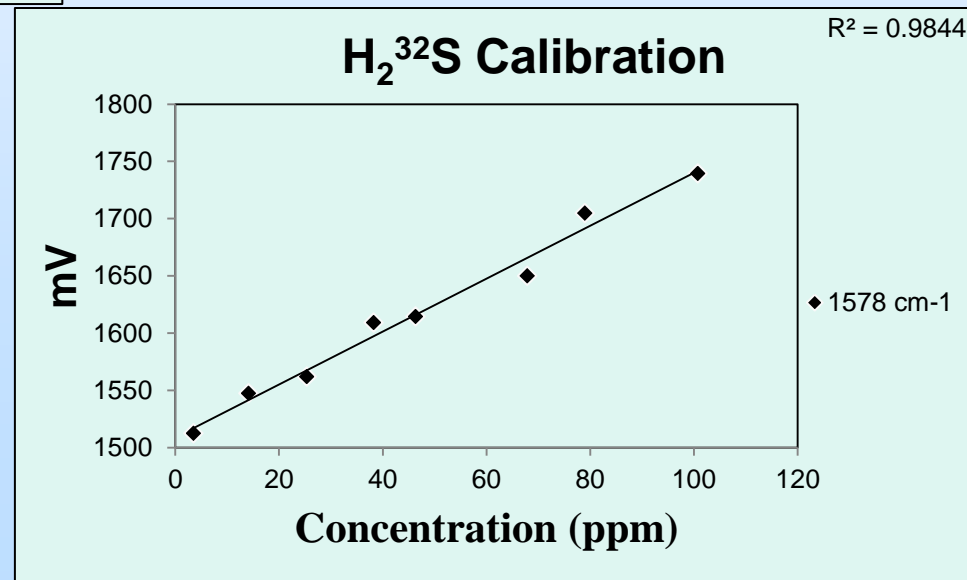
Estimated Detection Limit
 $^{12}\text{CH}_4$ and $^{13}\text{CH}_4 < 1$ ppb



Hydrogen Sulfide Calibration



Estimated Detection Limit
 $\text{H}_2^{32}\text{S} < 1 \text{ ppb}$

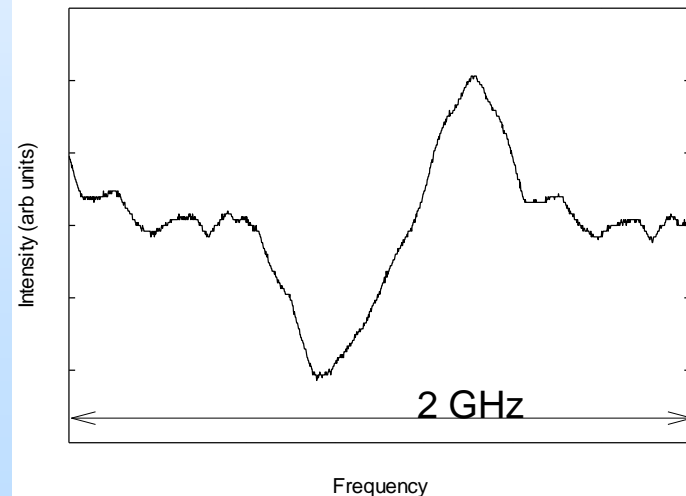


LIDAR Instrument

Added CH₄ and H₂S detection to CO₂ LIDAR instrument



- Direct a CW Laser Across Sequestration Site
- 10ns Modulator Pulse
- Record Time Resolved Return Signal
- Convert Time to Distance



Improving velocity models for microseismic imaging

- **Motivation**

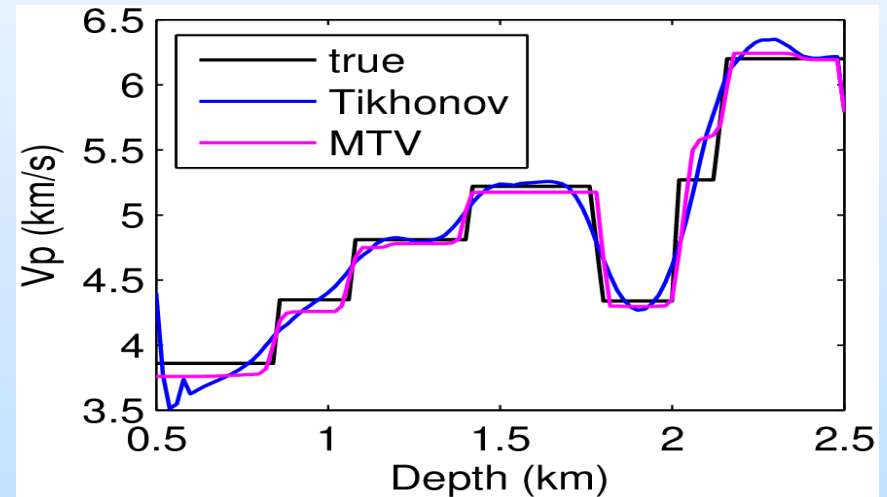
- Accurate velocity models are needed for locating microseismic events and inverting focal mechanisms.

- **Objective**

- Develop a new velocity inversion method termed fat-ray double-difference tomography with a modified total-variation regularization scheme, to improve velocity inversion

- **Validation**

- Demonstrate with synthetic microseismic data that our new method improves velocity inversion.



The velocity model reconstructed with our new method (MTV) (red) is more accurate than that inverted using the conventional Tikhonov regularization technique (blue). The black curve is the true velocity model.

Improving velocity models for microseismic imaging with a sparse seismic network

- **Motivation**

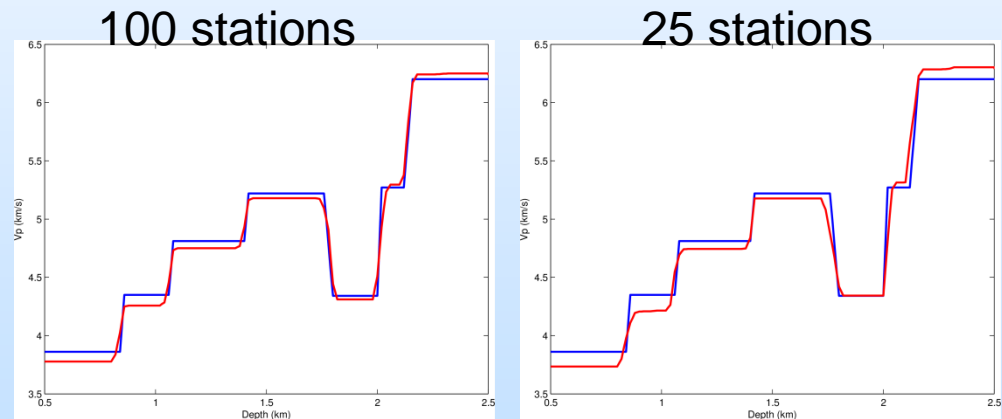
- To improve velocity inversion for sparsely distributed seismic stations.

- **Objective**

- Develop a new velocity inversion method termed double-difference tomography with a compressive sensing technique, to improve velocity inversion

- **Validation**

- Demonstrate with synthetic microseismic data that our new method can handle sparse seismic network.



The velocity model reconstructed using all seismic stations (red line in the left panel) has similar accuracy as that inverted using only a quarter of all stations (red line in the right panel). The blue curve is the true velocity model.

Improving microseismic event locations for monitoring CO₂ inject at the Aneth EOR field

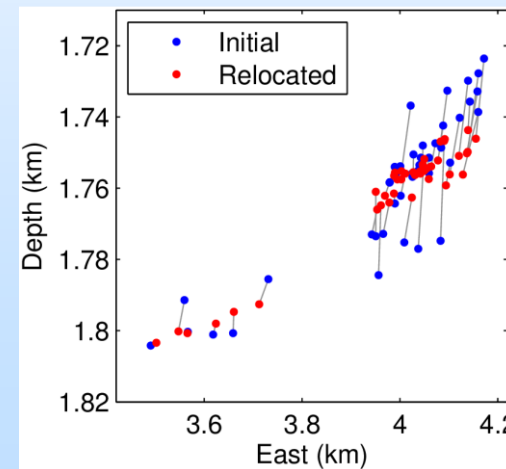
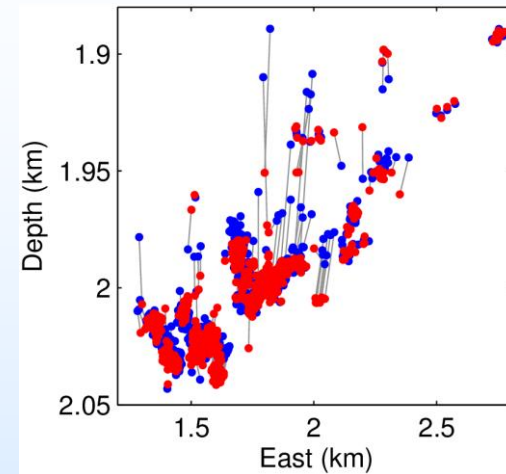
- **Motivation**

- To obtain high-precision locations of microseismic events.

- **Objective**

- Apply our newly developed fat-ray double-difference tomography algorithm to microseismic data acquired for monitoring CO₂ injection at the Aneth EOR field to improve event locations.

Microseismic data were recorded using a 23-level borehole geophone string.



The initial (blue dots) and relocated (red dots) microseismic event locations for two microseismic event clusters.

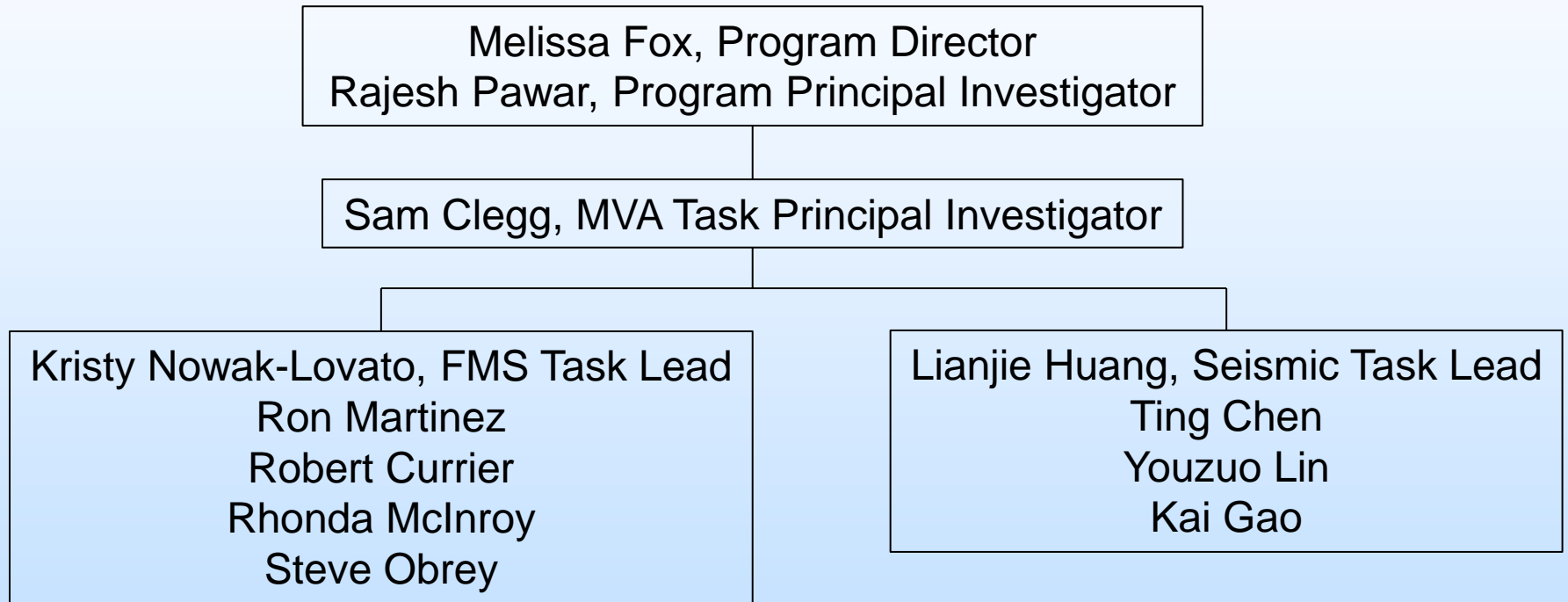
Accomplishments to Date

- Frequency Modulated Spectroscopy
 - Integrated CH₄ and H₂S detection into existing in situ CO₂ FMS instrument
 - ^{13/12}CH₄ detection to <1ppb
 - H₂³²S detection to <1ppb
 - Integrated CH₄ and H₂S detection into existing CO₂ LIDAR instrument
- Advanced Seismic Imaging
 - Developed two new methods to improve velocity models for microseismic imaging
 - Developed a new method for improving location precision of microseismic events and applied it to field data.

Summary

- Key Findings
 - FMS
 - $^{13/12}\text{CO}_2$, H_2 $^{34/32}\text{S}$ and $^{13/12}\text{CH}_4$ stable isotopes are sensitive signatures of seepage from carbon sequestration and EOR sites.
 - Detection of these stable isotope signatures can be integrated into the same instrument.
 - Advanced Seismic Imaging
 - New inversion algorithms can improve velocity models for microseismic imaging.
 - The location precision of microseismic events can be improved using a new method.
- Lessons Learned
 - Field experiment are critical tests to validate the instruments and algorithms developed under this program
- Future Plans
 - LIDAR instrument limited by available detector technologies. We will build a customized detector to maximize LIDAR sensitivity.
 - We will improve focal mechanism inversion of microseismic events.

Organization Chart



Bibliography

List peer reviewed publications generated from the project per the format of the examples below

- Journal, one author:

- Gaus, I., 2010, Role and impact of CO₂-rock interactions during CO₂ storage in sedimentary rocks: International Journal of Greenhouse Gas Control, v. 4, p. 73-89, available at: XXXXXXXX.com.

- Journal, multiple authors:

- MacQuarrie, K., and Mayer, K.U., 2005, Reactive transport modeling in fractured rock: A state-of-the-science review. Earth Science Reviews, v. 72, p. 189-227, available at: XXXXXXXX.com.
- Shang, X. and L. Huang, 2012. Optimal designs of time-lapse seismic surveys for monitoring CO₂ leakage through fault zones, International Journal of Greenhouse Gas Control, 10:419-433.
- Zhang, Z. and L. Huang, 2013. Double-difference elastic-waveform inversion with prior information for time-lapse monitoring, Geophysics, 78(6):R259-273.
- Tan, S. and L. Huang, 2014. An efficient finite-difference method with high-order accuracy in both time and space domains for modelling scalar-wave propagation, ²² Geophys. J. Int. 197, 1250-1267.

Bibliography

List peer reviewed publications generated from the project per the format of the examples below

- Journal, multiple authors (continued):
 - Tan, S. and L. Huang, 2014. A staggered-grid finite-difference scheme optimized in the time–space domain for modeling scalar-wave propagation in geophysical problems, *Journal of Computational Physics* 276, 613-634.
 - Lin, Y. and L. Huang, 2015. Acoustic- and elastic-waveform inversion using a modified total-variation regularization scheme, *Geophys. J. Int.* 200, 489-502.
- Publication:
 - Bethke, C.M., 1996, *Geochemical reaction modeling, concepts and applications*: New York, Oxford University Press, 397 p.
 - Chen, S. L. Huang and J. Rutledge, Locating microseismic events using fat-ray double difference tomography for monitoring CO2 injection at the Aneth EOR field, 2014 AGU Fall Meeting.
 - Lin, Y. and L. Huang, Double-Difference Waveform Inversion with a Modified Total-Variation Regularization Scheme: Application to Time-Lapse Walkaway VSP Data, 2014 AGU Fall Meeting.

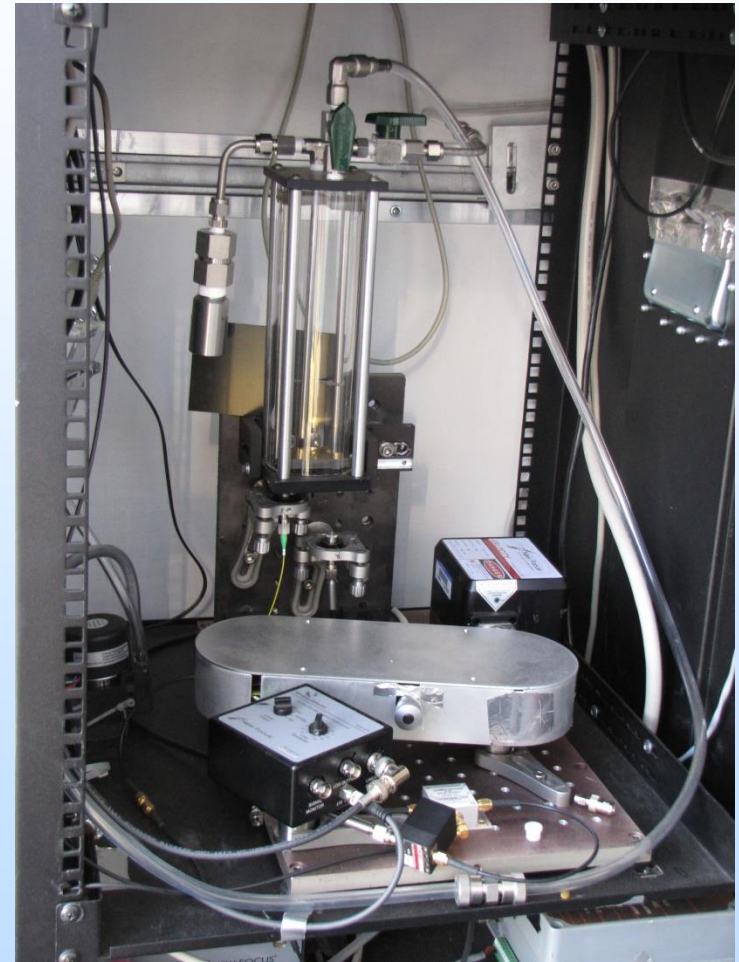
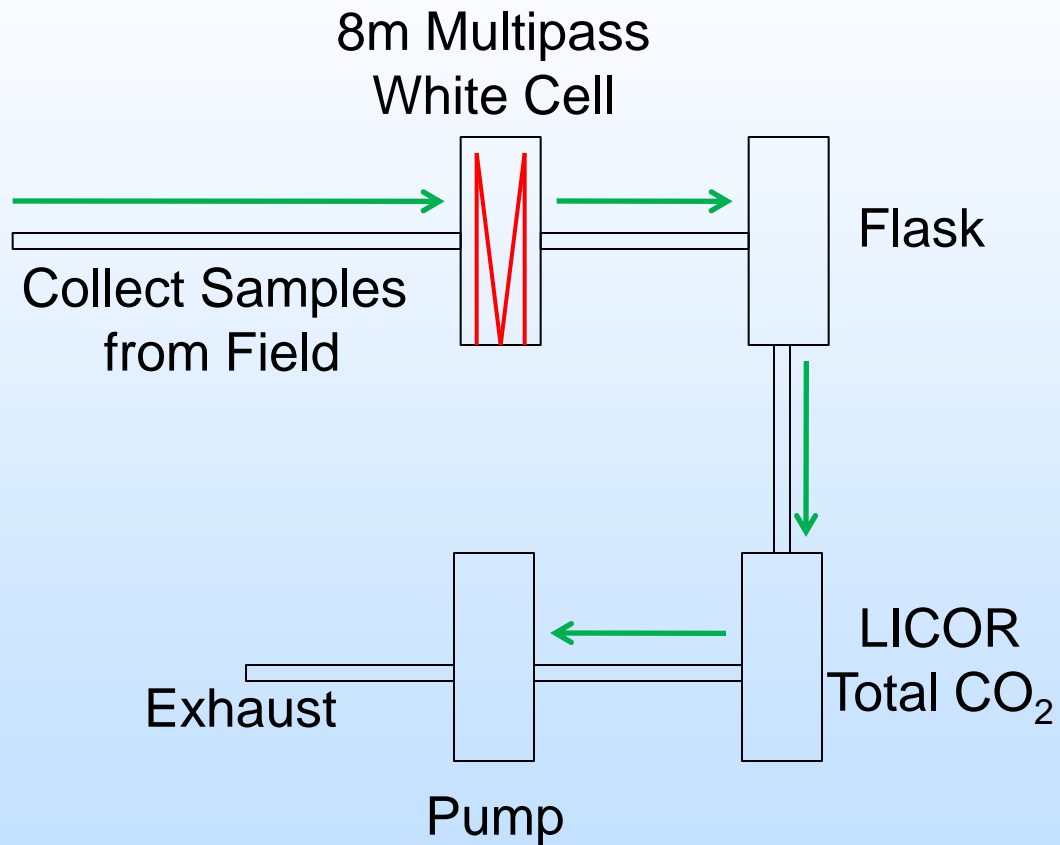
Bibliography

List peer reviewed publications generated from the project per the format of the examples below

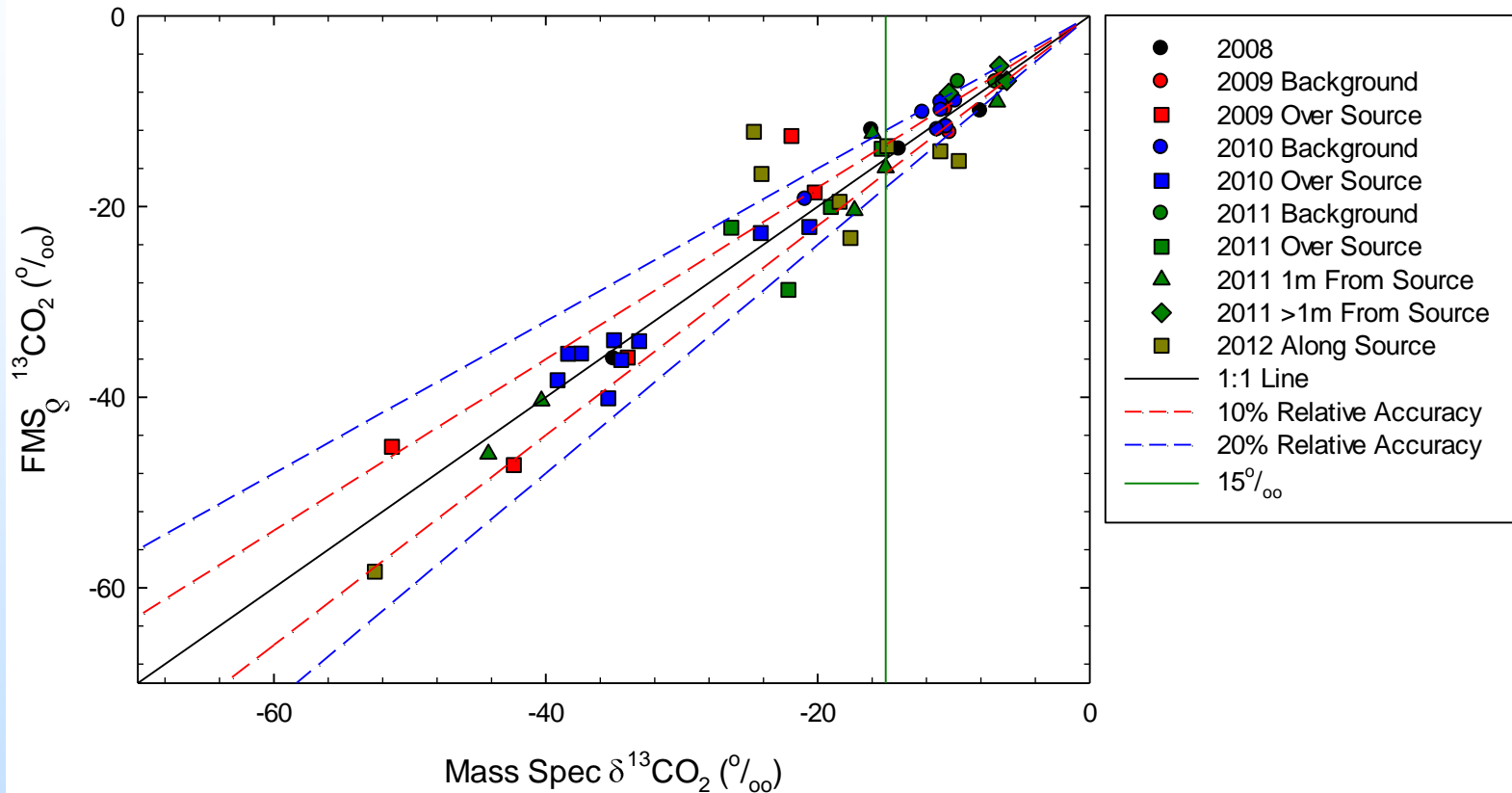
- Publication (continued):
 - Bethke, C.M., 1996, Geochemical reaction modeling, concepts and applications: New York, Oxford University Press, 397 p.
 - Chen, S. L. Huang and J. Rutledge, Locating microseismic events using fat-ray double difference tomography for monitoring CO2 injection at the Aneth EOR field, 2014 AGU Fall Meeting.
 - Lin, Y. and L. Huang, Double-Difference Waveform Inversion with a Modified Total-Variation Regularization Scheme: Application to Time-Lapse Walkaway VSP Data, 2014 AGU Fall Meeting.
 - Chen, S. and L. Huang, Improving microseismic velocity inversion using fat-ray double-difference tomography with a modified total-variation regularization scheme, 2015 CCUS Annual Conference.
 - Lin, Y., T. Chen, and L. Huang, Double-Difference Tomography with a Compressive Sensing Technique for Microseismic Imaging with a Sparse Seismic Network, 2015 CCUS Annual Conference.

backup

In Situ FMS Instrument



In Situ Observations

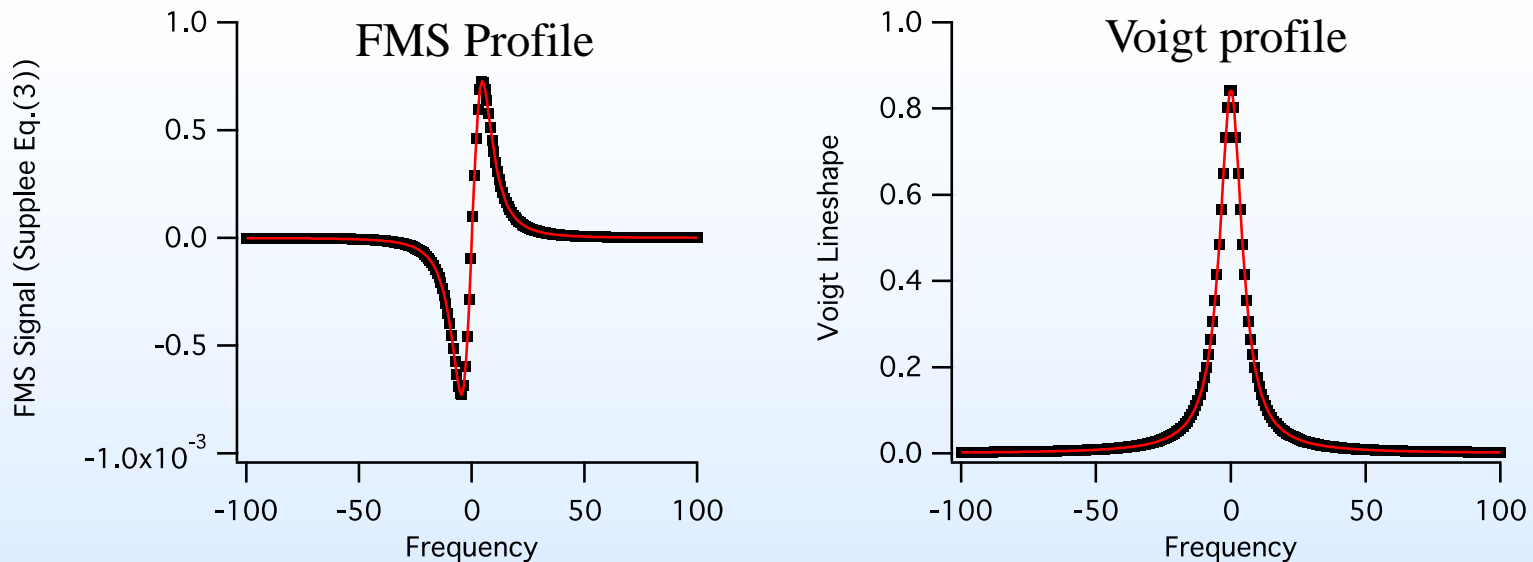


Historical Trends

Background $> -15^{\circ}/_{\text{oo}}$

Seepage $< -15^{\circ}/_{\text{oo}}$

Forward-Backward FMS Systems Model



- The Voigt profile shown on the right as black squares was used to generate simulated FMS signal as a function of carrier frequency (shown as black squares in the left-hand plot). The theoretical equation for the FMS signal was then fit to that simulated FMS signal.
- The resulting fit to the simulated FMS signal is shown as a red line in the left-hand plot.
- The Voigt line shape corresponding to the best-fit parameters determined during that regression is then shown as a red line on the right. It accurately reproduces the original Voigt feature.
- The agreement is excellent in both forward and backwards fitting. For this calculation, $M=0.1$ and $\omega_m=0.1$.